

# Seismic anisotropy beneath the Juan de Fuca plate system: Evidence for heterogeneous mantle flow

Miles Bodmer<sup>1</sup>, Douglas R. Toomey<sup>1</sup>, Emilie E. Hooft<sup>1</sup>, John Nábělek<sup>2</sup>, and Jochen Braunmiller<sup>3</sup>

<sup>1</sup>Department of Geological Sciences, University of Oregon, Eugene, Oregon 97403, USA

<sup>2</sup>College of Earth, Ocean and Atmospheric Sciences, Oregon State University, Corvallis, Oregon 97331-5503, USA

<sup>3</sup>School of Geosciences, University of South Florida, Tampa, Florida 33620-5550, USA

## ABSTRACT

Here we use SKS shear wave splitting observations from ocean-bottom seismometer data to infer patterns of mantle deformation beneath the Juan de Fuca plate and its adjoining boundaries. Our results indicate that the asthenosphere beneath the Juan de Fuca plate responds largely to absolute plate motion with an anisotropic layer developing rapidly near the ridge and persisting into the subduction zone. Geographically restricted deviations from this pattern indicate the presence of secondary processes. At discrete plate boundaries, such as the Blanco transform fault, seismic anisotropy is attributed to relative plate motion within a narrow zone (<50 km). Beneath the deforming southern Gorda plate region—a diffuse plate boundary—splitting observations similarly suggest deformation dominated by relative motion between the rigid Juan de Fuca and Pacific plates but distributed over a broad zone (~200 km). Our results are inconsistent with toroidal flow around the southern edge of the subducting slab due to rollback, as suggested by onshore studies. Instead, reorganization of upper mantle flow associated with plate fragmentation seems to dominate the anisotropic signature of southern Cascadia.

## INTRODUCTION

Mantle convection and the movement of tectonic plates drive flow in Earth's viscous upper mantle. The nature of mantle flow and its relation to plate boundary evolution are relevant to plate dynamics and thus remain topics of vigorous inquiry. Because mantle strain induces lattice preferred orientation of seismically anisotropic minerals, particularly olivine, seismic methods can be used to constrain patterns of mantle flow (Silver and Chan, 1991).

The Juan de Fuca (JdF) plate system is an excellent target for investigating the forces that drive oceanic mantle flow. In a compact region we find all three types of discrete plate boundaries, lithospheric plates that are both intact (JdF) and internally deforming (southern Gorda plate), and an evolving subduction zone system susceptible to edge effects, slab rollback, and plate fragmentation (Fig. 1). The Cascadia Initiative, a multiyear, onshore-offshore experiment (Toomey et al., 2014), and a complementary Blanco transform array (Ghorbani et al., 2015) specifically target these regions and for the first time provide dense coverage of an entire oceanic plate and its boundaries.

Here we use ocean bottom seismometer (OBS) data and the well-established shear wave splitting method to investigate mantle flow beneath the JdF plate system. Owing to the extensive coverage of our OBS array, and the spatial coherence of interstation shear wave splitting observations, we are able to detect significant heterogeneity in the oceanic mantle flow field. Our results have implications for the forces that drive asthenospheric flow and for the evolution of the complex plate interactions that define southern Cascadia.

## DATA AND METHODS

We analyze seismic data from five onshore Cascadia Initiative instruments, 117 OBS sites from years 1, 2, and 3 of the Cascadia Initiative, and

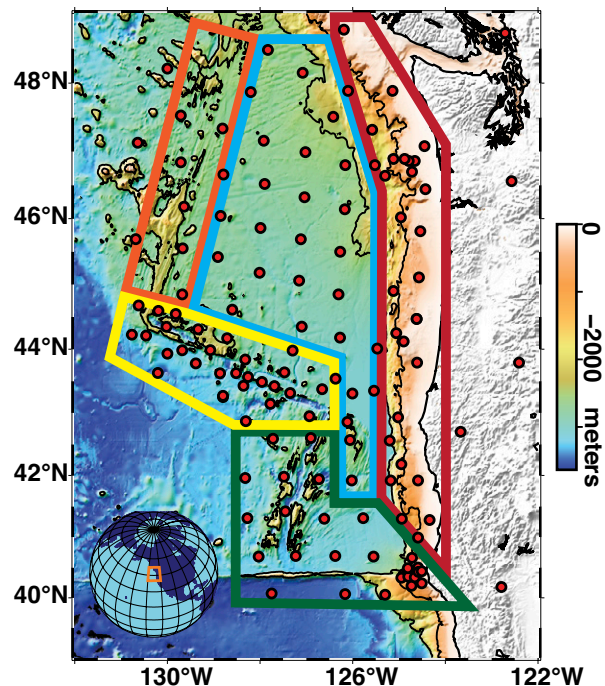


Figure 1. Bathymetric and topographic map showing location of seismometers (red circles) and geographic regions defined by tectonic setting and observed splitting patterns: blue—Juan de Fuca plate interior, red—Cascadia subduction zone, orange—Juan de Fuca Ridge, yellow—Blanco transform, green—Mendocino Triple Junction and southern Gorda region.

30 OBSs from the Blanco array (Fig. 1; Fig. DR1 in the GSA Data Repository<sup>1</sup>). The orientations of the horizontal components of the Cascadia Initiative OBSs were determined by Sumy et al. (2015) with a median uncertainty in channel orientation of  $\pm 9^\circ$  at the  $1\sigma$  confidence level. We analyze the SKS phase of teleseismic events,  $M_w \geq 6$ , at distances of  $90^\circ$ – $130^\circ$ . All onshore instruments and 111 of the 147 OBSs recorded at least one usable event (Table DR1 in the Data Repository). The OBSs recorded an average of four usable events, and only 14 sites recorded just a single usable event (Table DR2). Back-azimuthal event coverage is limited and has a westward bias for the OBS data due to the short deployment time (Fig. DR2).

We implemented a workflow that uses strict quality control to account for high environmental noise levels typical of OBS data. Our SKS splitting analysis was conducted using the Splitlab software package (Wüstefeld et al., 2008), which performs three common splitting methods: rotation correlation (RC) (Bowman and Ando, 1987), Silver and Chan (SC), and eigenvalue (EV) (Silver and Chan, 1991). Each method estimates the polarization direction of the fast shear wave  $\Phi$  and the delay time  $\delta t$  between the fast and slow shear waves (Fig. DR3). Initial measurements are filtered

<sup>1</sup>GSA Data Repository item 2015365, Tables DR1 and DR2 (splitting parameters and event list), and Figures DR1–DR6 (enlarged station map, backazimuthal distribution of events, examples of the waveforms analyzed, dependence on plate age, variation of splitting parameters by backazimuth, and two-layer anisotropy models), is available online at [www.geosociety.org/pubs/ft2015.htm](http://www.geosociety.org/pubs/ft2015.htm), or on request from [editing@geosociety.org](mailto:editing@geosociety.org) or Documents Secretary, GSA, P.O. Box 9140, Boulder, CO 80301, USA.

with a third-order, zero-phase Butterworth bandpass filter (0.03–0.1 Hz). This isolates the SKS arrival within a relatively low noise band between the microseism peak (0.1–2 Hz) and the high-frequency limit of infragravity waves (<0.04 Hz). Measurements are repeated for several filter limits adjusted between 0.02 and 0.15 Hz and covering at least a full octave. Multiple measurements allow for a qualitative assessment of stability from which a final event measurement is chosen; reported measurements often include higher frequencies, even those that may obscure the previously identified SKS waveform, improving accuracy (Restivo and Helffrich, 1999). We report measurements using only the SC method due to the poor performance of the RC method on low signal-to-noise data (Vecsey et al., 2008). All three methods are used for quality control, verifying that results from the SC and EV methods are consistent and that the RC method is either consistent or yields results indicative of high noise contamination (Vecsey et al., 2008). Measurements with delay times >3.5 s or <0.5 s are discarded. Possible null measurements are not reported because they are indistinguishable from measurements with high noise levels on the transverse channel.

Maps of the transverse energy are generated by grid searching in the  $\delta t$ - $\Phi$  parameter space. A single set of splitting parameters is estimated for each station by stacking the normalized energy maps (Wolfe and Silver, 1998) and a statistical F-test is applied to obtain the 95% confidence intervals (Fig. DR3) (Silver and Chan, 1991), which are converted to  $1\sigma$  errors. Typical uncertainties in  $\Phi$  and  $\delta t$  are  $8^\circ$  and 0.3 s (Table DR1), respectively, although in shallow water they tend to be larger. To verify that we can recover known splitting parameters, we analyzed good quality data from onshore Cascadia Initiative stations and successfully reproduced the trench perpendicular pattern found by previous studies (e.g., Eakin et al., 2010).

## RESULTS

Our SKS splitting results (Figs. 2 and 3) reveal spatially coherent patterns in fast polarization directions that are correlated with five tectonic environments (Fig. 1): (1) the JdF plate interior and northern Gorda plate; (2) the southern, internally deforming Gorda plate and Mendocino Triple Junction (MTJ); (3) the Juan de Fuca Ridge; (4) the Cascadia subduction zone (CSZ); and (5) the Blanco transform fault.

The fast polarization directions within the JdF plate interior and the northern Gorda plate show an average trend of  $N63^\circ E$  that extends from 50 km east of the ridge to the subduction zone (Figs. 2 and 3A). Delay times are 1 s, on average, and do not appear to vary with plate age (Fig. DR4). Orientations correlate poorly with the JdF plate–Pacific plate spreading direction ( $N107^\circ E$ ). To estimate the absolute plate motion (APM) of the JdF plate, we use the APM of the Pacific plate, which is well known, and the Pacific–JdF relative plate motion (RPM) calculated from the MORVEL model (DeMets et al., 2010). In this reference frame, fast polarization directions broadly correlate with APM ( $N30^\circ E$  to  $N50^\circ E$ , depending on location; see Fig. 3A). We note, however, that the observed fast polarization directions are systematically rotated clockwise from the APM direction (Fig. 3A).

In the southern Gorda plate, we observe a region of coherent fast polarization measurements oriented  $N109^\circ E$  (Figs. 2 and 3B). This trend extends beyond the Gorda plate into the Pacific plate, and is not disrupted by the Gorda spreading center or the Mendocino transform fault. The northern boundary of this region correlates well with the onset of intense lithospheric deformation of the southern Gorda plate (Chaytor et al., 2004). Measurements within 25 km of the MTJ show large variance but become consistent at greater distances (Fig. 3B). In contrast to the JdF plate interior, the observed fast polarization directions are inconsistent with the JdF APM. Although similar to the APM of the Pacific plate ( $N122^\circ E$ ) and the relative spreading direction of the southern Gorda Ridge ( $N98^\circ E$ ), fast polarization directions agree best with the relative motion between the non-deforming JdF and Pacific plates ( $N107^\circ E$ ). Delay times are 1.4 s on average with low variability and do not appear to have any spatial dependence.

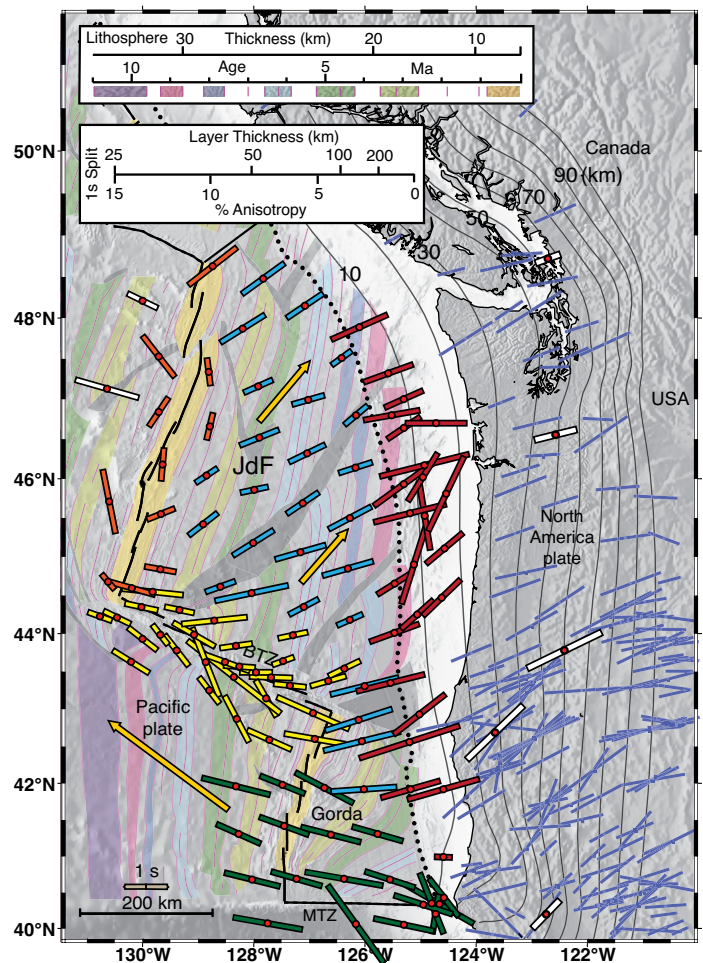


**Figure 2. SKS splitting results overlaying magnetic anomalies (light colored bands) and propagator wakes (gray bands) (from Nedimović et al., 2009; Wilson 1988, 1993). Thick bars indicate our measurements color coded by zone (see Fig. 1). Orientation of a bar shows the fast polarization direction; its length is scaled by the delay time. Yellow arrows are the absolute plate motions (modified from MORVEL; DeMets et al., 2010). Blue bars are SKS splitting measurements from land studies (Currie et al., 2004; Eakin et al., 2010; Bonnin et al., 2010). Thin black lines are depth to slab contoured at 10 km intervals (McCrorry et al., 2012). Top scale (upper left) shows the sea floor age and corresponding lithospheric thickness for a half-space cooling model; the bottom scale shows layer thicknesses and percent anisotropy for a 1 s delay time. JdF—Juan de Fuca region; MTJ—Mendocino transform zone; BTZ—Blanco transform zone.**

Measurements within 50 km of the Juan de Fuca Ridge are sparse and suggest a variable pattern (Figs. 2 and 3C). Near the intersection of the Juan de Fuca Ridge and Blanco transform fast polarization directions correlate with JdF–Pacific RPM. Throughout most of the central ridge segments there appears to be a broad ridge-parallel trend, most notably near the Axial Seamount, that diminishes northward. Average delay times are 1 s.

Near the CSZ, most fast polarization directions closely resemble those within the JdF plate interior and the western United States (Figs. 2 and 3D) and delay times are 1.4 s on average. The relative convergence of the JdF plate and North America is at  $N56^\circ E$  and the trench orientation changes from  $\sim N2^\circ W$  to  $N48^\circ W$ , from south to north. Relative to the trench trend, measurements in the southern and northern CSZ are roughly trench perpendicular but rotate counterclockwise toward trench parallel between  $44^\circ N$  and  $46^\circ N$ . The region of trench-parallel orientations coincides with several geologic features that make central Cascadia anomalous, e.g., where subduction changes orientation and flattens (McCrorry et al., 2012).

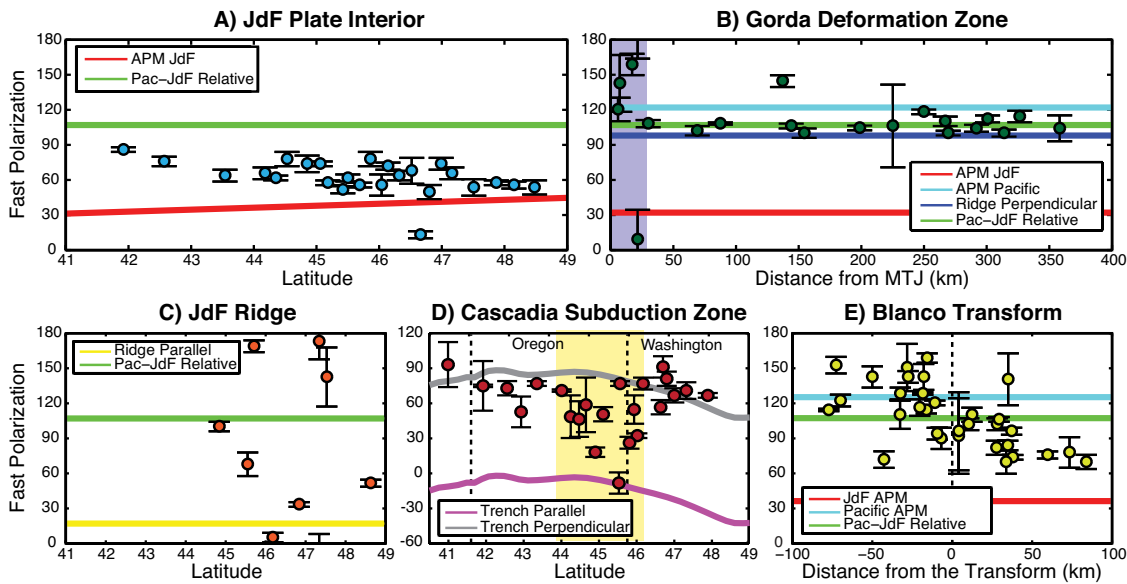


**Figure 3.** Plots of the fast polarization direction (degrees clockwise from north) as a function of distance or latitude for each of the zones shown in Figure 1; measurements (circles) are color coded by zone (see Fig. 1). Colored lines show orientations predicted by various scenarios. Purple band (B) represents the region within 25 km of the Mendocino Triple Junction (MTJ) and the yellow band (D) is the region of anomalous observations in central Cascadia. JdF—Juan de Fuca; Pac—Pacific; APM—absolute plate motion.

In the Blanco transform region fast polarization directions rapidly change from northwest-southeast to northeast-southwest when crossing the transform from the Pacific to JdF plates and correlate well with respective APMs (Figs. 2 and 3E). Within 25 km of the transform, orientations parallel the relative motion of the JdF and Pacific plates. Delay times are 1 s on average.

## DISCUSSION

We use our splitting results to infer regional-scale patterns of mantle flow by assuming that the observed fast polarization directions are sub-parallel to the direction of maximum shear (e.g., Silver and Chan, 1991). Our data are insufficient to explicitly test for multiple anisotropic layers (see Figs. DR5 and DR6); however, we consider the possibility of depth-dependent anisotropy in our interpretations. Sites with only one or two measurements are less certain, but the observations are supported by their consistency with neighboring sites. Given 4% mantle anisotropy, a splitting time of ~1 s would require an ~100-km-thick anisotropic layer. Because our split times are typically 1 s or more, and predicted lithospheric thickness in this region is 5–30 km (Fig. 2), we infer that the bulk of observed anisotropy originates in the asthenosphere.

We attribute anisotropy beneath the JdF and northern Gorda plates to an entrained layer of asthenosphere influenced by APM and altered by a secondary process. Subslab entrainment has been interpreted for several Cascadia data sets (Currie et al., 2004; Eakin et al., 2010; Bonnin et al., 2010), young subduction zones (Lynner and Long, 2014), and geodynamic models (Faccenda and Capitanio, 2012). Correlation with APM in the JdF plate interior and the CSZ (Figs. 3A and 3D) is consistent with the plate dragging asthenosphere into the subduction zone via viscous coupling. The systematic clockwise rotation of fast polarization directions from APM suggests that some secondary process is important. One possibility is that a shallow layer of anisotropy aligned with RPM due to corner flow at the ridge results in an apparent fast axis altered by multiple layering. However, this requires an ~0.5 s delay time contribution, implying either a very thick (50 km at 4% anisotropy) or highly anisotropic (12% at 20 km thickness) layer (Fig. DR6). While anisotropy related to plate spreading is very likely, it is unclear whether it exists in the necessary magnitudes. Furthermore, most observations near the ridge are inconsistent with the RPM direction. An alternative interpretation is that asthenospheric flow is also driven by internal convection unrelated to APM. Indeed, seismic studies of the Endeavor segment of the Juan de Fuca Ridge show that subridge mantle divergence is skewed clockwise with respect to the plate

spreading direction and related to a recent change in JdF-Pacific plate motion (VanderBeek et al., 2014).

At the Blanco transform, a discrete plate boundary between the JdF and Pacific plates, we infer a narrow shear zone with deformation aligned with RPM. Rapid changes in fast polarization orientations across the transform indicate highly localized deformation within a 50-km-wide zone centered on the transform. The distribution of strain with depth is unknown; however, relatively low viscosities in the asthenosphere beneath the transform and/or very shallow anisotropic structure may be necessary to produce the rapid changes in orientation observed, particularly when considering the overlap of SKS Fresnel zones.

Beneath the southern Gorda plate region, a diffuse plate boundary, we attribute anisotropy to a broad shear zone accommodating Pacific-JdF RPM (Figs. 3B and 4). In response to northward movement of the Pacific plate, the southern Gorda lithosphere is undergoing internal deformation, which is evident in bathymetry (Fig. 1), magnetic anomalies (Fig. 2), anomalous orientations of the Gorda Ridge and Mendocino transform, bookshelf faulting (Chaytor et al., 2004), and geodynamic models of regional stress (Wang et al., 1997). Correlation of our observations with both the region of crustal deformation and the Pacific-JdF RPM suggests a common causal factor for both lithospheric and asthenospheric deforma-

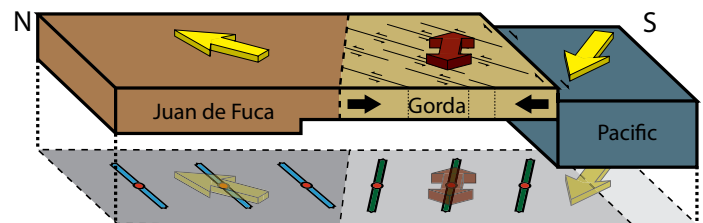


**Figure 4.** Schematic of upper mantle anisotropy beneath the Juan de Fuca (JdF) plate interior and the southern Gorda region. Top layer: yellow arrows indicate absolute plate motions. The red double arrow represents the relative motions of the Pacific-JdF plates. Black arrows represent north-south compression of southern Gorda plate region. Small black arrows depict the Mendocino transform fault and strike-slip faulting within the southern Gorda plate. Bottom layer: typical splitting orientations color coded by zone (see Fig. 1); fast polarization directions beneath the JdF plate are rotated clockwise from absolute plate motion and within the southern Gorda plate region are parallel to Pacific plate–JdF plate relative motion.

tion. In our proposed model (Fig. 4) the southern Gorda region is a weak zone separating two rigid plates and thus accommodates the relative motion between them with both asthenosphere and lithosphere undergoing deformation and upper mantle strain aligned with RPM. Our results, in conjunction with those near the Explorer plate (Mosher et al., 2014), suggest that reorientation of upper mantle flow plays a critical role in plate fragmentation, with RPM alignment beneath the Gorda plate representing an intermediate state before full detachment.

Our results are inconsistent with the rollback-induced toroidal flow model commonly invoked for onshore anisotropy near the MTJ (e.g., Zandt and Humphreys, 2008). Geodynamic models suggest that beneath a downgoing plate toroidal flow results in strong trench-parallel deformation (Faccenda and Capitanio, 2012), which is inconsistent with our results by  $\sim 65^\circ$  (Figs. 2 and 3B). Furthermore, observed orientations and delay times do not vary with distance from the slab edge and abruptly change orientation at the northern limits of the Gorda deformation zone. We conclude that there is no large-scale toroidal flow due to slab rollback or that the deformation is weak resulting in minimal influence on measurements. Diversion of ambient flow around the southern slab edge is another possible source of deformation (Eakin et al., 2010). However, due to the lack of variation with distance from the slab edge, large delay times, and correlations with Gorda plate deformation we assert that its contribution to the anisotropic structure is, if present, secondary.

## CONCLUSIONS

Seismic anisotropy of the upper mantle beneath the JdF plate system is remarkably heterogeneous, indicating that a variety of forces drive flow in the oceanic asthenosphere. Beneath rigid plates, APM is a significant driver of flow that entrains asthenosphere and drags it into subduction zones. There is also evidence of a secondary source of anisotropy possibly related to non-APM convective processes. Near plate boundaries anisotropy records relative plate motion (e.g., Blanco), but in some cases is complex (e.g., Juan de Fuca Ridge and Mendocino transform). Plate fragmentation occurring within the diffuse plate boundary in the southern Gorda plate region is accompanied by reorganization of upper mantle flow.

## ACKNOWLEDGMENTS

We thank S. Carbotte and two anonymous reviewers for thoughtful comments. This work was supported by National Science Foundation grants OCE-1139701 and OCE-1333196 to the University of Oregon and grant OCE-1031858 to Oregon State University.

## REFERENCES CITED

Bonnin, M., Barruol, G., and Bokelmann, G.H., 2010, Upper mantle deformation beneath the North American–Pacific plate boundary in California from SKS splitting: *Journal of Geophysical Research*, v. 115, B04306, doi:10.1029/2009JB006438.

Bowman, J.R., and Ando, M., 1987, Shear-wave splitting in the upper-mantle wedge above the Tonga subduction zone: *Geophysical Journal International*, v. 88, p. 25–41, doi:10.1111/j.1365-246X.1987.tb01367.x.

Chaytor, J.D., Goldfinger, C., Dziak, R.P., and Fox, C.G., 2004, Active deformation of the Gorda plate: Constraining deformation models with new geophysical data: *Geology*, v. 32, p. 353–356, doi:10.1130/G20178.2.

Currie, C.A., Cassidy, J.F., Hyndman, R.D., and Bostock, M.G., 2004, Shear wave anisotropy beneath the Cascadia subduction zone and western North American craton: *Geophysical Journal International*, v. 157, p. 341–353, doi:10.1111/j.1365-246X.2004.02175.x.

DeMets, C., Gordon, R.G., and Argus, D.F., 2010, Geologically current plate motions: *Geophysical Journal International*, v. 181, p. 1–80, doi:10.1111/j.1365-246X.2009.04491.x.

Eakin, C.M., Obrebski, M., Allen, R.M., Boyarko, D.C., Brudzinski, M.R., and Porritt, R., 2010, Seismic anisotropy beneath Cascadia and the Mendocino triple junction: Interaction of the subducting slab with mantle flow: *Earth and Planetary Science Letters*, v. 297, p. 627–632, doi:10.1016/j.epsl.2010.07.015.

Faccenda, M., and Capitanio, F.A., 2012, Development of mantle seismic anisotropy during subduction-induced 3-D flow: *Geophysical Research Letters*, v. 39, L11305, doi:10.1029/2012GL051988.

Ghorbani, P., Nabelek, J., and Braunmiller, J., 2015, Gorda and Juan de Fuca plate seismicity recorded by the Cascadia Initiative and Blanco transform fault zone seismic arrays [abs.]: *Seismological Research Letters*, v. 86, p. 682, doi:10.1785/0220150017.

Lynner, C., and Long, M.D., 2014, Testing models of sub-slab anisotropy using a global compilation of source-side shear wave splitting data: *Journal of Geophysical Research*, v. 119, p. 7226–7244, doi:10.1002/2014JB010983.

McCrorry, P.A., Blair, J.L., Waldhauser, F., and Oppenheimer, D.H., 2012, Juan de Fuca slab geometry and its relation to Wadati-Benioff zone seismicity: *Journal of Geophysical Research*, v. 117, B09306, doi:10.1029/2012JB009407.

Mosher, S.G., Audet, P., and L'Heureux, I., 2014, Seismic evidence for rotating mantle flow around subducting slab edge associated with oceanic microplate capture: *Geophysical Research Letters*, v. 41, p. 4548–4553, doi:10.1002/2014GL060630.

Nedimović, M.R., Bohnenstiehl, D.R., Carbotte, S.M., Canales, J.P., and Dziak, R.P., 2009, Faulting and hydration of the Juan de Fuca plate system: *Earth and Planetary Science Letters*, v. 284, p. 94–102, doi:10.1016/j.epsl.2009.04.013.

Restivo, A., and Helffrich, G., 1999, Teleseismic shear wave splitting measurements in noisy environments: *Geophysical Journal International*, v. 137, p. 821–830, doi:10.1046/j.1365-246x.1999.00845.x.

Silver, P.G., and Chan, W.W., 1991, Shear wave splitting and subcontinental mantle deformation: *Journal of Geophysical Research*, v. 96, p. 16,429–16,454, doi:10.1029/91JB00899.

Sumy, D.F., Lodewyk, J.A., Woodward, R.L., and Evers, B., 2015, Ocean-bottom seismograph performance during the Cascadia Initiative: *Seismological Research Letters*, v. 86, doi:10.1785/0220150110.

Toomey, D.R., et al., 2014, The Cascadia initiative: A sea change in seismological studies of subduction zones: *Oceanography*, v. 27, p. 138–150, doi:10.5670/oceanog.2014.49.

VanderBeek, B.P., Toomey, D.R., Hooft, E.E.E., and Wilcock, W.S.D., 2014, Segment-scale seismic structure of slow-, intermediate-, and fast-spreading mid-ocean ridges: Constraints on the origin of ridge segmentation and the geometry of shallow mantle flow: *American Geophysical Union Fall Meeting*, abs. V23E-07.

Vecsey, L., Plomerová, J., and Babuška, V., 2008, Shear-wave splitting measurements—Problems and solutions: *Tectonophysics*, v. 462, p. 178–196, doi:10.1016/j.tecto.2008.01.021.

Wang, K., He, J., and Davis, E.E., 1997, Transform push, oblique subduction resistance, and intraplate stress of the Juan de Fuca plate: *Journal of Geophysical Research*, v. 102, no. B1, p. 661–674, doi:10.1029/96JB03114.

Wilson, D.S., 1988, Tectonic history of the Juan de Fuca ridge over the last 40 million years: *Journal of Geophysical Research*, v. 93, p. 11,863–11,876, doi:10.1029/JB093iB10p11863.

Wilson, D.S., 1993, Confidence intervals for motion and deformation of the Juan de Fuca plate: *Journal of Geophysical Research*, v. 98, p. 16,053–16,071, doi:10.1029/93JB01227.

Wolfe, C.J., and Silver, P.G., 1998, Seismic anisotropy of oceanic upper mantle: Shear wave splitting methodologies and observations: *Journal of Geophysical Research*, v. 103, p. 749–771, doi:10.1029/97JB02023.

Wüstefeld, A., Bokelmann, G., Zaroli, C., and Barruol, G., 2008, SplitLab: A shear-wave splitting environment in Matlab: *Computers & Geosciences*, v. 34, p. 515–528, doi:10.1016/j.cageo.2007.08.002.

Zandt, G., and Humphreys, E., 2008, Toroidal mantle flow through the western US slab window: *Geology*, v. 36, p. 295–298, doi:10.1130/G24611A.1.

Manuscript received 20 July 2015

Revised manuscript received 14 October 2015

Manuscript accepted 20 October 2015

Printed in USA